Asian Journal of Chemistry; Vol. 27, No. 6 (2015), 2055-2060

ASIAN JOURNAL OF CHEMISTRY

http://dx.doi.org/10.14233/ajchem.2015.17688

Synthesis and Properties of Nano-Sized $ZnWO_4:Eu^{3+}$ Phosphors by Hydrothermal Method

YONG-QING ZHAI*, XUAN LI, RUI-FANG LI, JIN-HANG LI and YUE DONG

College of Chemistry and Environmental Science, Hebei University, Baoding 071002, P.R. China

*Corresponding author: E-mail: zhaiyongqinghbu@163.com

Received: 29 March 2014; *Accepted*: 28 May 2014; *Published online*: 17 March 2015; AJC-16959

$ZnWO_4:Eu^{3+}$ phosphors were synthesized by the hydrothermal method at different conditions. The phase structure, morphology and luminescent properties of the as-synthesized samples were characterized by X-ray diffraction, scanning electron microscope and fluorescence spectrophotometer, respectively. The results indicate that all of the $ZnWO_4:Eu^{3+}$ phosphors are pure monoclinic structure. The $ZnWO_4:Eu^{3+}$ samples are spherical nanoparticles and the particle size of samples increases a little with increasing the hydrothermal temperature and time. The excitation spectrum of $ZnWO_4:Eu^{3+}$ shows a broad excitation band extending from 220 to 350 nm and a series of sharp excitation peaks between 350 and 500 nm. The emission spectrum of the sample $ZnWO_4:Eu^{3+}$ under the excitation at 301 nm is composed of the weak broad band attributing to the intrinsic emission of WO_4^{2-} groups and a series of sharp emission peaks originating from the characteristic emission of Eu^{3+}. The emission intensity of Eu^{3+} at 616 nm reaches the strongest when the pH value is 6, the hydrothermal temperature is 180 °C, the hydrothermal time is 12 h and the Eu^{3+} concentration is 2 mol. % under the excitation at 301 nm. Meanwhile, it is found that the emission intensity of Eu^{3+} at 616 nm reach the highest when Eu^{3+} concentration is 6 mol. % under the excitation at 395 and 465 nm. Moreover, the photoluminescence colour of the sample can be tuned from blue, white and orange to red by adjusting the relative doping concentrations of Eu^{3+} in $ZnWO_4:Eu^{3+}$.

Keywords: Phosphors, $ZnWO_4:Eu^{3+}$, Hydrothermal method, Luminescence.

INTRODUCTION

Metal tungstates are very important inorganic functional materials widely used in various fields, such as photoluminescent materials, scintillators, optical fibers, photocatalysts, gas and humidity sensors, *etc*[1-5]. According to the ionic radius of the cations, the divalent metal tungstates AWO_4 are divided into two types of structures *i.e.*, Wolframite structure and Scheelite structure[6,7]. Tungstates with relatively smaller cations like Zn^{2+}, Mg^{2+}, Ni^{2+} and Co^{2+} (ionic radius < 0.77 Å) form the wolframite structure with the tungsten in octahedral coordination. Whereas tungstates with larger cations like Ba^{2+}, Ca^{2+}, Sr^{2+} and Pb^{2+} (ionic radius > 0.99 Å) form the Scheelite structure with $[WO_4]$ tetrahedron. Among all of them, $ZnWO_4$ possesses the monoclinic Wolframite structure with space group P2/c.

In rare earth-doped $ZnWO_4$ phosphors, WO_4^{2-} as a kind of self-activating ions can emit bright blue-green lights under UV excitation[8,9] and the WO_4^{2-} can absorb and efficiently transfer energy to rare earths ions. Therefore, the luminescent materials of rare earth-doped $ZnWO_4$ attract extensive attention. For example, Dong *et al.*[10] prepared $ZnWO_4$ and $ZnWO_4:Eu^{3+}$ by the self-propagating combustion method. They also analyzed the luminescent properties of samples and their photocatalytic activity in the degradation of rhodamine-B. Liao *et al.*[11] prepared $ZnWO_4:Tb^{3+}$ phosphors *via* the hydrothermal method and investigated the luminescence properties of phosphors by adding different charge compensators. Li *et al.*[12] synthesized $ZnWO_4:Tb^{3+}$ and $ZnWO_4:Eu^{3+}$ spherical nanoparticles by hydrothermal method and studied the influences of trivalent rare earth concentration on photoluminescence properties. He[13] prepared $ZnWO_4$ and $ZnWO_4:Sm^{3+}$ powders by wet chemical method and systematically analyzed the effects of calcination temperature on the photoluminescence properties.

In this paper, $ZnWO_4:Eu^{3+}$ phosphors were synthesized by a facile hydrothermal method and the effects of pH value, hydrothermal temperature, hydrothermal time and Eu^{3+} concentration on the phase structure, morphology and luminescent properties of $ZnWO_4:Eu^{3+}$ phosphors were also investigated.

EXPERIMENTAL

Eu_2O_3 (99.99 %), $Na_2WO_4{\cdot}2H_2O$, $Zn(NO_3)_2{\cdot}6H_2O$, HNO_3 and NaOH were employed as the starting materials. They were all analytical reagents (A.R.) and used without any further purification.

The $ZnWO_4:Eu^{3+}$ phosphors were synthesized by a facile hydrothermal process. The specific procedure is as follows.

First, Eu_2O_3 was dissolved in a certain amount of nitric acid to form $Eu(NO_3)_3$ aqueous solution. The accurate concentration of $Eu(NO_3)_3$ solution was 0.1929 mol/L, determined by EDTA complexing titrimetry. Second, $ZnWO_4$:6 mol. % Eu^{3+} is taken as an example. 1.957 g $Zn(NO_3)_2{\cdot}6H_2O$ was dissolved in 20 mL deionized water to form $Zn(NO_3)_2$ aqueous solution and then 2.18 mL $Eu(NO_3)_3$ solution was introduced into it with continuous stirring to make the solution mix uniformly. Meanwhile, 2.309 g $Na_2WO_4{\cdot}2H_2O$ was dissolved in 30 mL deionized water to form Na_2WO_4 aqueous solution and then the Na_2WO_4 solution was dropped into the above mixed solution under magnetic stirring. The white suspension was formed. The HNO_3 or NaOH solution was added dropwise into the reaction system to adjust the pH value at 5, 6 and 8. After stirring for 0.5 h, the solution was transferred into a Teflon-lined stainless steel autoclave of 100 mL capacity with a filling capacity of 80 %. The autoclave was sealed and maintained at a series of temperatures in the range of 140-200 °C for 12 h and at 180 °C for a series of hydrothermal times in the range of 6-18 h in an oven. After air-cooled to room temperature, the as-synthesized white precipitates were filtered and washed with deionized water and absolute ethanol three times, respectively. Finally, the obtained product was dried in the oven at 90 °C for 6 h. A series of $ZnWO_4$:xEu^{3+} (x = 0, 0.5, 2, 4, 8 mol. %) were prepared by the above similar process.

Phase structure and crystallization of the samples were carried out on a Y-2000 X-ray powder diffraction (XRD) with CuK_α radiation (30 kV × 20 mA and λ = 1.54178 Å). The morphology of the phosphors was analyzed with a JSM-7500F field emission scanning electron microscopy (FE-SEM). Fluorescence spectra of the samples were measured on an F-380 fluorescence spectrometer and the excitation and emission slits were 10 and 5 nm, respectively. All measurements were conducted at room temperature.

RESULTS AND DISCUSSION

XRD analysis: In order to investigate the effects of pH value, hydrothermal temperature, hydrothermal time and Eu^{3+} concentration on phase structure, a series of samples were hydrothermally synthesized under different conditions, and their XRD patterns are shown in Figs. 1-4, respectively. It can be seen that all of the diffraction peaks are easily indexed to a pure monoclinic wolframite structure with space group P2/c and additional peaks cannot be found, indicating that Eu^{3+} ions have introduced into the $ZnWO_4$ host lattice and have little effect on the phase structure of $ZnWO_4$.

Fig. 1 shows that the intensity of the diffraction peaks increases significantly and the diffraction peaks become sharper with the pH value increasing from 5 to 6. However, it also shows that a further increase of the pH value to 8 leads to the decrease of the intensity of the diffraction peaks.

Fig. 2 shows that the intensity of diffraction peaks increases gradually with the increase of temperature from 140 to 180 °C, revealing that the crystallinity of the sample is enhanced gradually. However, the intensity of diffraction peaks decreases a little when the temperature reached to 200 °C.

From Fig. 3, it is clear that the intensity of diffraction peaks increases a little with the increase of hydrothermal time from 6 to 12 h and the intensity of peaks remain almost the same when the hydrothermal time is more than 12 h.

From Fig. 4, it can be seen that the diffraction peaks of the samples are shifted to lower degree with the increase of

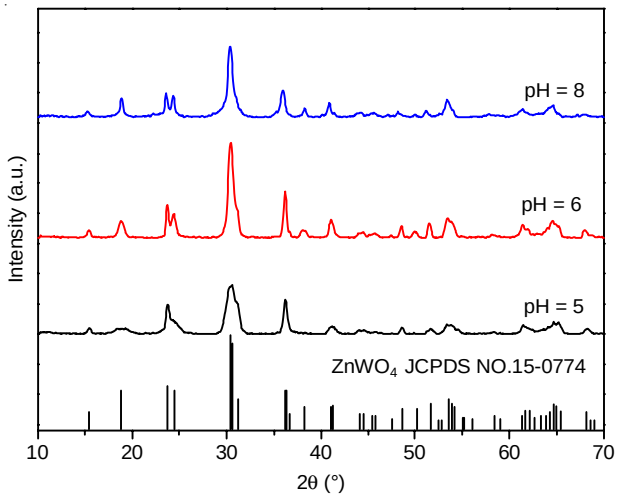

Fig. 1. XRD patterns of $ZnWO_4$:6%Eu^{3+} powders prepared at 180 °C for 12 h with different pH values

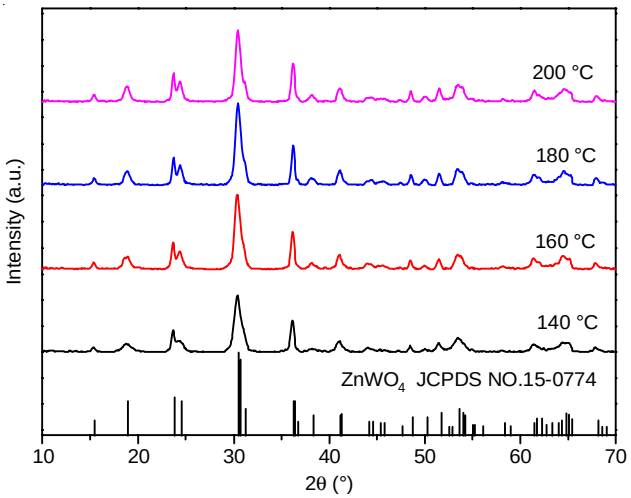

Fig. 2. XRD patterns of $ZnWO_4$:6%Eu^{3+} powders prepared at different hydrothermal temperature for 12 h with pH = 6

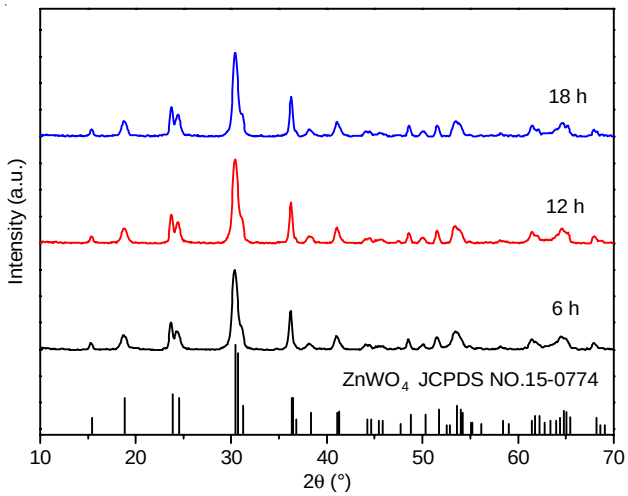

Fig. 3. XRD patterns of $ZnWO_4$:6%Eu^{3+} powders prepared at 180 °C for different hydrothermal time with pH = 6

Eu^{3+} concentration. The reason is as follows. The relative ionic radius of Eu^{3+} (0.95 Å) is close to that of Zn^{2+} (0.74 Å), but larger than that of W^{6+} (0.62 Å)[9]. Meanwhile, the charge of Eu^{3+} is close to that of Zn^{2+}. Hence, Eu^{3+} ions prefer to locate in Zn^{2+} sites. According to Bragg's equation, $2d\sin\theta = \lambda$, θ decreases gradually with the increase of d. Among them, d represents interplanar spacing, θ represents Bragg angle and λ is the wavelength of X-ray (λ = 1.54178 Å). Because the radius of Eu^{3+} is larger than that of Zn^{2+}, the interplanar spacing d of samples increases gradually as the doping concentration of Eu^{3+} increases, so Bragg angle θ decrease, *i.e.*, the peaks are moved to lower angle.

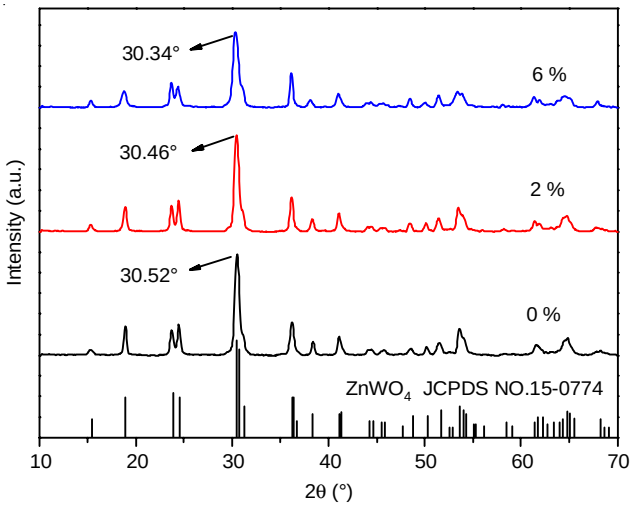

Fig. 4. XRD patterns of the $ZnWO_4:Eu^{3+}$ powders with different Eu^{3+} concentration prepared at 180 °C for 12 h (pH = 6)

SEM analysis: In order to investigate the morphology and particle size of the samples, the SEM images of the synthesized $ZnWO_4$:6%Eu^{3+} phosphors at different conditions with pH = 6 are shown in Fig. 5. It can be seen that all the $ZnWO_4:Eu^{3+}$ samples present spherical nanoparticles. The particle edge of sample prepared at 140 °C for 12 h is not clear and the particle size is the smallest (about 30-55 nm), indicating that the crystallinity is low, which is consistent with the XRD results. The particle edge of sample prepared at 180 °C for 6 h is clear and the particle size is about 40-65 nm. The particle size of sample synthesized at 180 °C for 12 h is the largest and about 40-70 nm. Therefore, it can be concluded that increasing the hydrothermal temperature and time leads to the small increase of particle size of the samples.

Excitation and emission spectrum: For the $ZnWO_4:Eu^{3+}$ phosphors synthesized at different conditions, the shape of excitation and emission spectra are similar. $ZnWO_4$:6%Eu^{3+} sample prepared at 180 °C for 12 h with pH = 6 is taken as an example. The excitation and emission spectrum is shown in Fig. 6. It can be seen that the excitation spectrum (left part) not only includes a broad excitation band extending from 220 to 350 nm with the peak wavelength at 301 nm, but also a series of sharp excitation peaks between 350 and 500 nm. The broad excitation band is ascribed to the charge transfer transition (CT) of W-O and Eu-O. The sharp excitation peaks are attributed to the f-f transition of Eu^{3+} and the strong excitation peaks are located at 395 and 465 nm corresponding to $^7F_0 \rightarrow {}^5L_6$ and $^7F_0 \rightarrow {}^5D_2$ transition of Eu^{3+}, respectively.

The corresponding emission spectrum (right part) of $ZnWO_4$:6%Eu^{3+} under the excitation at 301 nm is shown in Fig. 6. It indicates that the emission spectrum is consisted of two parts: the weak broad band ranging from 350 to 550 nm attributing to the intrinsic emission of WO_4^{2-} groups and a series of sharp emission peaks originating from the characteristic emission of Eu^{3+}. In the second part, three emission peaks located at 594, 616 and 658 nm, are ascribed to the magnetic dipole transition of $^5D_0 \rightarrow {}^7F_1$, the electronic dipole transition of $^5D_0 \rightarrow {}^7F_2$ and radiative transition of $^5D_0 \rightarrow {}^7F_3$, respectively. Generally, Eu^{3+} ion is a good probe to test the crystal field environmental of the rare earth ions[9], because the electronic dipole transition is sensitive to the local symmetry, while the magnetic dipole transition is insensitive to the surrounding environment. When the Eu^{3+} ion occupies a site with an inversion symmetry center, the $^5D_0 \rightarrow {}^7F_1$ transition is relatively strong, resulting in orange-red emitting around 594 nm. Conversely, if Eu^{3+} ion occupies a site without an inversion center, the hypersensitive $^5D_0 \rightarrow {}^7F_2$ transition is dominating, resulting in red emitting around 616 nm. As shown in Fig. 6, the strongest emission peak of $ZnWO_4:Eu^{3+}$ phosphor is located at 616 nm and the red to orange (R/O) intensity ratio ($I_{616\ nm}/I_{594\ nm}$) is very large. Therefore, it can be suggest that Eu^{3+} ions mainly occupy the sites without inversion symmetry center.

Effects of pH value on luminescent properties: Fig. 7 shows the emission spectra of $ZnWO_4$:6%Eu^{3+} powders prepared at 180 °C for 12 h with different pH values. It is observed that the pH value has little effect on the position of the peaks, but has great effect on the intensity of emission peaks. The emission intensity goes highest when pH = 6. The possible reason is as follows. When the pH value is 6, the crystallinity of samples

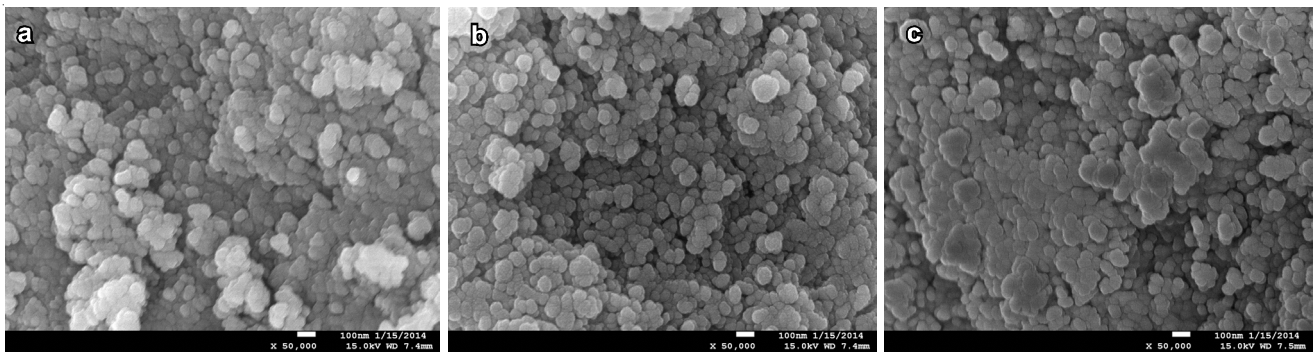

Fig. 5. SEM images of samples obtained at (a) 140 °C for 12 h, (b) 180 °C for 6 h and (c) 180 °C for 12 h

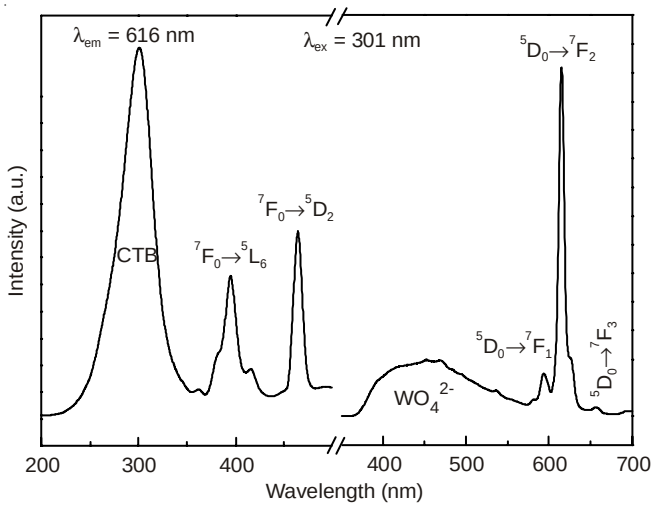

Fig. 6. Excitation spectrum (left part) and emission spectrum (right part) of $ZnWO_4$:6%Eu^{3+}

turns highest (Fig. 1) while the surface defects of particles become the least, leading to a decrease in the number of non-radiative transition, so the luminescent intensity is strongest. Therefore, it can be concluded that the appropriate pH value of the reaction system is 6.

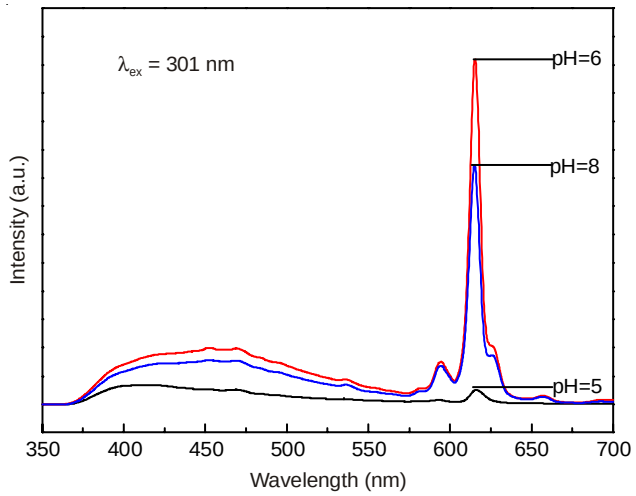

Fig. 7. Emission spectra of $ZnWO_4$:6%Eu^{3+} powders prepared at different pH values

Effects of hydrothermal temperature and time on luminescent properties: Fig. 8 presents the emission spectra of $ZnWO_4$:6%Eu^{3+} powders synthesized at different hydrothermal temperatures for 12 h with pH = 6. In the spectra, no visible shift of the position of emission peaks is observed. It is clear that in the scope of 140 to 180 °C, the intensity of the emission peaks noticeably increases with increasing the hydrothermal temperature, but the intensity of the emission peaks decreases when the temperature is more than 180 °C. The possible reason is that higher temperature causes the damage of the particles and decreases the crystallinity of the particles[14]. This phenomenon is consistent with the Fig. 2. Therefore, the optimum hydrothermal temperature is 180 °C.

The influence of hydrothermal time on the luminescent properties is also studied. The emission spectra of the $ZnWO_4$:6%Eu^{3+} samples obtained at 180 °C for different

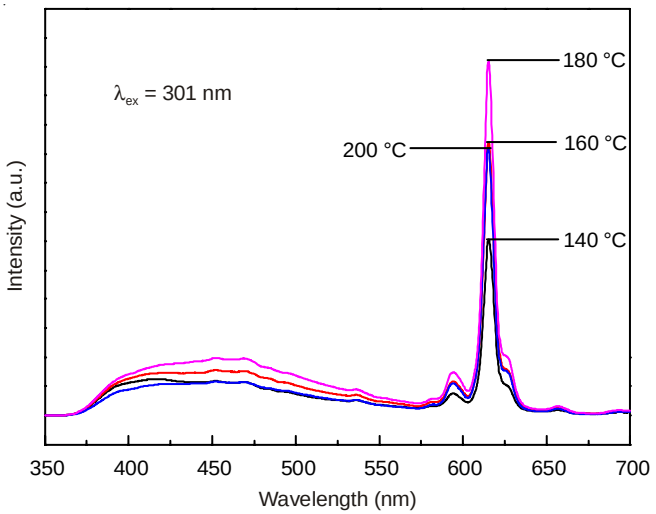

Fig. 8. Emission spectra of $ZnWO_4$:6%Eu^{3+} powders prepared at different hydrothermal temperature for 12 h

hydrothermal times with pH = 6 are shown in Fig. 9. In comparison with Fig. 8, it is interesting to observe that the influence of hydrothermal time is less important than that of hydrothermal temperature on the luminescent properties of samples. The intensity of the emission peaks increases a little as the hydrothermal time increases from 6 to 12 h and the intensity remains almost the same when the time is more than 12 h. Therefore, from the point of energy conservation, 12 h was chosen as the appropriate hydrothermal time.

Effect of Eu^{3+} concentration on luminescent properties: The excitation spectra of the $ZnWO_4$:xEu^{3+} (x = 0, 0.5, 2, 4, 6, 8 mol.%) powders prepared at 180 °C for 12 h with pH = 6 are showed in Fig. 10. For the pure $ZnWO_4$, a broad excitation band ranging from 200 to 350 nm can be found when monitored at 465 nm, which is ascribed to the charge transfer transition of O→W. In addition to the pure $ZnWO_4$, it can be seen that the shape and position of excitation spectra have no considerably change as the concentration of Eu^{3+} varies under the 616 nm monitoring. The excitation spectra of $ZnWO_4$:xEu^{3+} (x = 0.5, 2, 4, 6, 8 mol.%) are composed of two parts, A and B. The part A are the broad bands extending from 220 to 350 nm with the peak at 301 nm and the part B are a series of sharp peaks in the range of 350 to 500 nm with the peak at 395 and 465 nm. However, the intensities of excitation peaks vary remarkably with the increase of Eu^{3+} concentration. It is interesting to observe that the intensity orders of the part A and part B are different as the Eu^{3+} concentration varies and the higher concentration of Eu^{3+} leads to the decrease of excitation peak at 301 nm and the increase of excitation peak at 395 and 465 nm. The intensity of the excitation peak at 301 nm is the highest when the Eu^{3+} concentration is 2 mol.% and the intensity of excitation peak at 395 and 465 nm reach the maximum when x = 6 mol.%.

As shown in Fig. 10, the excitation spectra of $ZnWO_4$:xEu^{3+} (x = 0.5, 2, 4, 6, 8 mol.%) cover a wide region from 200 to 500 nm with the peak at 301, 395 and 465 nm. The phosphors can match well with UV-LED chip (~301 nm), NUV InGaN chip (~395 nm) and blue-LED chip (~465 nm). Therefore, the phosphors have an extensive application.

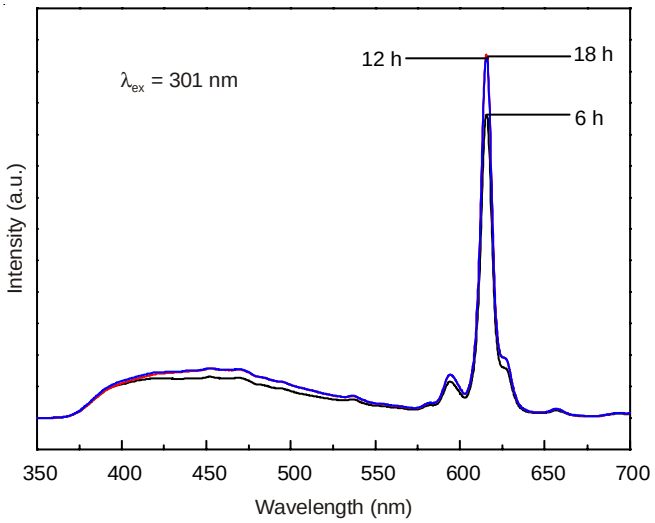

Fig. 9. Emission spectra of $ZnWO_4$:6%Eu^{3+} powders prepared at different hydrothermal time at 180 °C

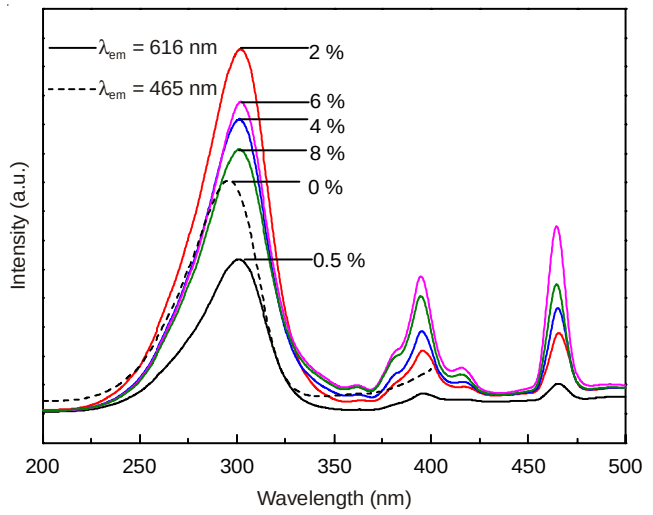

Fig. 10. Excitation spectra of $ZnWO_4:xEu^{3+}$ powders with different Eu^{3+} concentration

The corresponding emission spectra of the samples $ZnWO_4:xEu^{3+}$ (x = 0, 0.5, 2, 4, 6, 8 mol.%) prepared at 180 °C for 12 h with pH = 6 under the excitation at 301, 395 and 465 nm are shown in Figs. 11, 12 and 13, respectively. It is obvious that the shape and position of emission peaks has little shift with the increasing Eu^{3+} concentration in the three figures. From Fig. 11, in addition to the pure $ZnWO_4$, it can be seen that all the emission spectra can be consisted of two major parts, C and D. Part C are the WO_4^{2-} emission bands ranging from 350 to 550 nm and part D are the sharp characteristic emissions of Eu^{3+} between 550 and 700 nm. The higher the concentration of Eu^{3+} is, the weaker the luminescence intensity of the WO_4^{2-} is. This is because the WO_4^{2-} absorbs energy from the excitation at 301 nm and efficiently transfers it to Eu^{3+}. However, the luminescence intensity of part D increases remarkably with the increasing Eu^{3+} concentration from 0 to 2 mol.% and reaches the maximum at x = 2 mol.%. If the Eu^{3+} concentration x > 2 mol.%, the luminescence intensity of part D begins to decrease, which is the concentration quenching phenomenon[15].

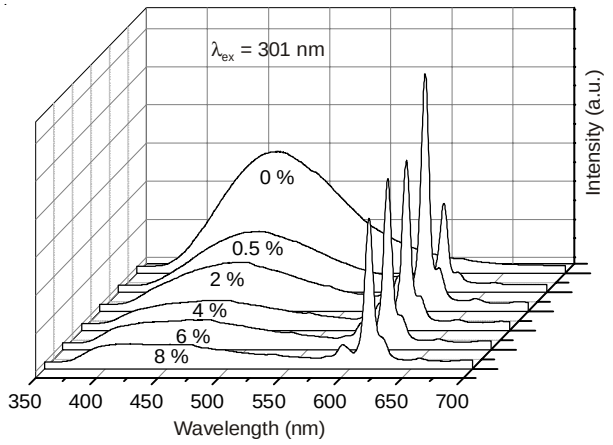

Fig. 11. Emission spectra (λ_{ex} = 301 nm) of $ZnWO_4:xEu^{3+}$ powders with different Eu^{3+} concentration

From Fig. 12 and 13, it can be seen that under the excitation of 395 and 465 nm, the intensities of emission peaks increase gradually as the Eu^{3+} concentration increases from 0.5 to 6 mol.% and the emission intensity reach the highest when x = 6 mol.%, indicating the concentration quenching occurs when the Eu^{3+} concentration is more than 6 mol.%.

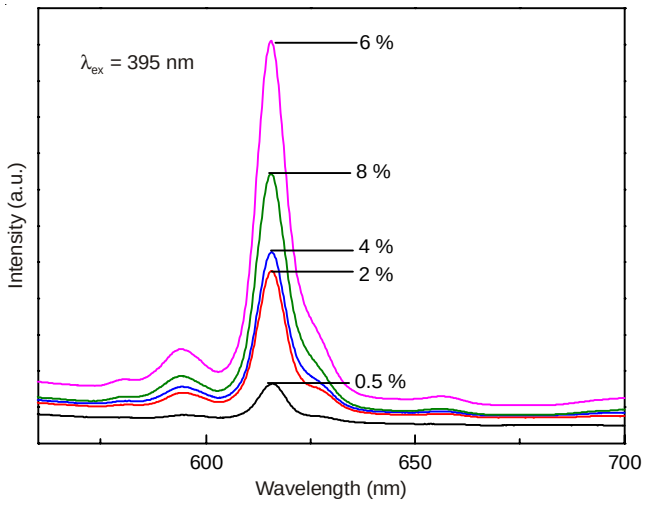

Fig. 12. Emission spectra (λ_{ex} = 395 nm) of $ZnWO_4:xEu^{3+}$ powders with different Eu^{3+} concentration

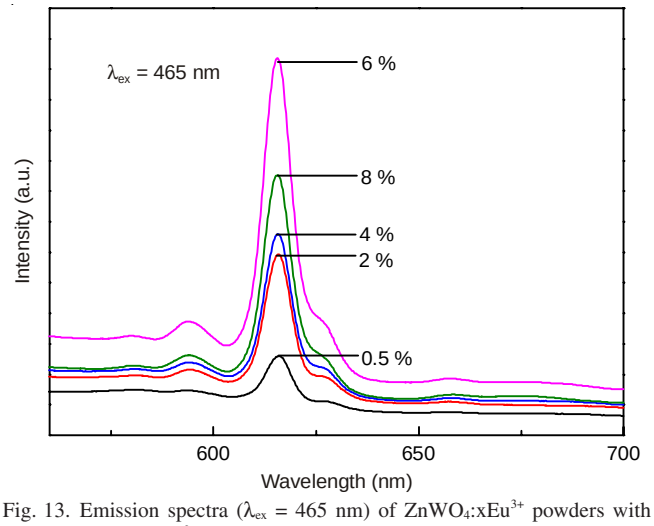

Fig. 13. Emission spectra (λ_{ex} = 465 nm) of $ZnWO_4:xEu^{3+}$ powders with different Eu^{3+} concentration

The CIE chromaticity diagram of $ZnWO_4:xEu^{3+}$ (x = 0, 0.5, 2, 4, 6, 8 mol.%) is shown in Fig. 14. The corresponding colour coordinates are determined to be (x = 0.223, y = 0.283), (x = 0.367, y = 0.302), (x = 0.530, y = 0.318), (x = 0.544, y = 0.323), (x = 0.583, y = 0.326), (x = 0.604, y = 0.328), respectively. According to the CIE diagram, it can be seen that the colour region shifts from blue region (point a) through white region (point b), orange region (point c, d) and finally to red region (point e, f) as the Eu^{3+} concentration increases. In particular, the point b (x = 0.5 mol.%) is close to the standard white chromaticity (x = 0.33, y = 0.33) for the National Television Standard Committee system[9]. Therefore, these $ZnWO_4:xEu^{3+}$ phosphors can be potentially used as phosphors in white lighting-emitting diodes (w-LEDs).

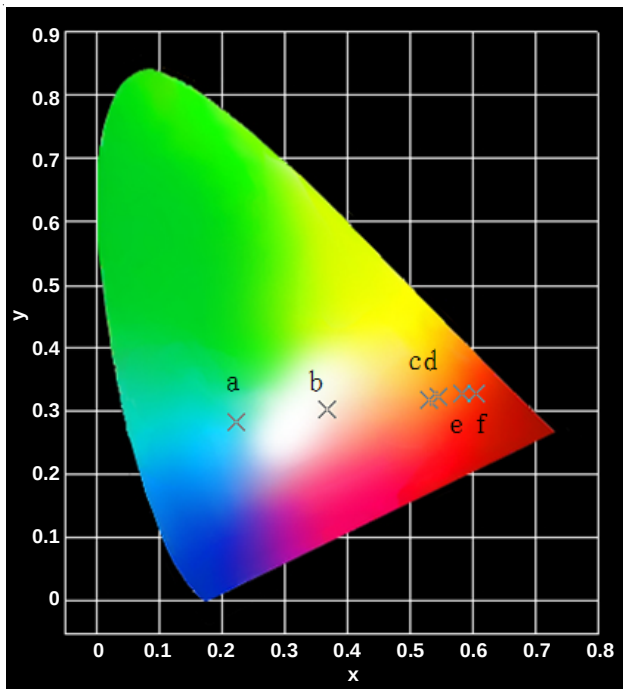

Fig. 14. CIE chromaticity diagram of $ZnWO_4:xEu^{3+}$ phosphors (a) x = 0, (b) x = 0.5, (c) x = 2, (d) x = 4, (e) x = 6, (f) x = 8

Conclusion

The $ZnWO_4:Eu^{3+}$ phosphors were synthesized successfully by the hydrothermal method. Compared with other methods, the hydrothermal method possesses the following advantages: mild reaction conditions, well dispersed particles, easy control of morphology, *etc*. All the as-synthesized $ZnWO_4:Eu^{3+}$ phosphors have the pure monoclinic phase with space group P2/c. The sample has better crystallinity when the pH value is 6, the hydrothermal temperature is 180 °C and the hydrothermal time is 12 h. The particles of the samples are spherical in shape and the size grows a little with increasing the hydrothermal temperature and time. For the samples $ZnWO_4:xEu^{3+}$ (x = 0, 0.5, 2, 4, 6, 8 mol.%), the emission intensity of the WO_4^{2-} decreases with the increase of the concentration of Eu^{3+}, while the emission intensity of Eu^{3+} first increase, then decrease. Under the excitation at 301 nm, the emission intensity of Eu^{3+} at 616 nm reaches the strongest when the Eu^{3+} concentration is 2 mol.%; under the excitation at 395 and 465 nm, it reaches the highest when Eu^{3+} concentration is 6 mol.%. The photoluminescence colour of the sample can be tuned from blue, white and orange to red by changing the relative doping concentrations of Eu^{3+} in $ZnWO_4:Eu^{3+}$. In particular, the colour coordinate of the sample $ZnWO_4:xEu^{3+}$ (x = 0.5 mol.%) is close to the standard white chromaticity (x = 0.33, y = 0.33), so $ZnWO_4:0.005Eu^{3+}$ can be potentially used as phosphors in white lighting-emitting diodes.

ACKNOWLEDGEMENTS

This study was supported by National Natural Science Foundation of China (No. 50672020).

REFERENCES

1. T. Montini, V. Gombac, A. Hameed, L. Felisari, G. Adami and P. Fornasiero, *Chem. Phys. Lett*., **498**, 113 (2010).
2. D.W. Kim, I.S. Cho, S.S. Shin, S. Lee, T.H. Noh, D.H. Kim, H.S. Jung and K.S. Hong, *J. Solid State Chem*., **184**, 2103 (2011).
3. S.M. Montemayor and A.F. Fuentes, *Ceram. Int*., **30**, 393 (2004).
4. S.J. Naik and A.V. Salker, *Solid State Sci*., **12**, 2065 (2010).
5. G.B. Kumar, K. Sivaiah and S. Buddhudu, *Ceram. Int*., **36**, 199 (2010).
6. S.H. Yoon, D.W. Kim, S.Y. Cho and K.S. Hong, *J. Eur. Ceram. Soc*., **26**, 2051 (2006).
7. K.M. Garadkar, L.A. Ghule, K.B. Sapnar and S.D. Dhole, *Mater. Res. Bull*., **48**, 1105 (2013).
8. Q.L. Dai, H.W. Song, X. Bai, G.H. Pan, S.Z. Lu, T. Wang, X.G. Ren and H.F. Zhao, *J. Phys. Chem. C*, **111**, 7586 (2007).
9. X.P. Chen, F. Xiao, S. Ye, X.Y. Huang, G.P. Dong and Q.Y. Zhang, *J. Alloys Comp*., **509**, 1355 (2011).
10. T.T. Dong, Z.H. Li, Z.X. Ding, L. Wu, X.X. Wang and X.Z. Fu, *Mater. Res. Bull*., **43**, 1694 (2008).
11. J.S. Liao, D. Zhou, X. Qiu, S.H. Liu and H.R. Wen, *Optik-Int. J. Light Electron Opt*, **124**, 5057 (2013).
12. C.Y. Li, X.D. Du, D. Yue, J.N. Gao and Z.L. Wang, *Mater. Lett*., **108**, 257 (2013).
13. H.Y. He, *Phys. Status Solidi B*, **246**, 177 (2009).
14. H.B. Fu, J. Lin, L.W. Zhang and Y.F. Zhu, *Appl. Catal. A*, **306**, 58 (2006).
15. F.S. Wen, X. Zhao, H. Huo, J.S. Chen, E. Shu-Lin and J.-H. Zhang, *Mater. Lett*., **55**, 152 (2002).